Electronic Supplementary Information (ESI)

A Self-powered, One-step Chip for Rapid, Quantitative and Multiplex Detection of Proteins from Pin-pricks of Whole Blood

Jun Wang, Habib Ahmad, Chao Ma, Qihui Shi, Ophir Vermesh, Udi Vermesh & James Heath*

NanoSystems Biology Cancer Center, Kavli Nanoscience Institute, Division of Chemistry and Chemical Engineering, California Institute of Technology, MC 127-72, 1200 E. California Blvd., Pasadena, California, 91125, USA.

**Correspondence should be addressed to J.R.H. (heath@caltech.edu).*
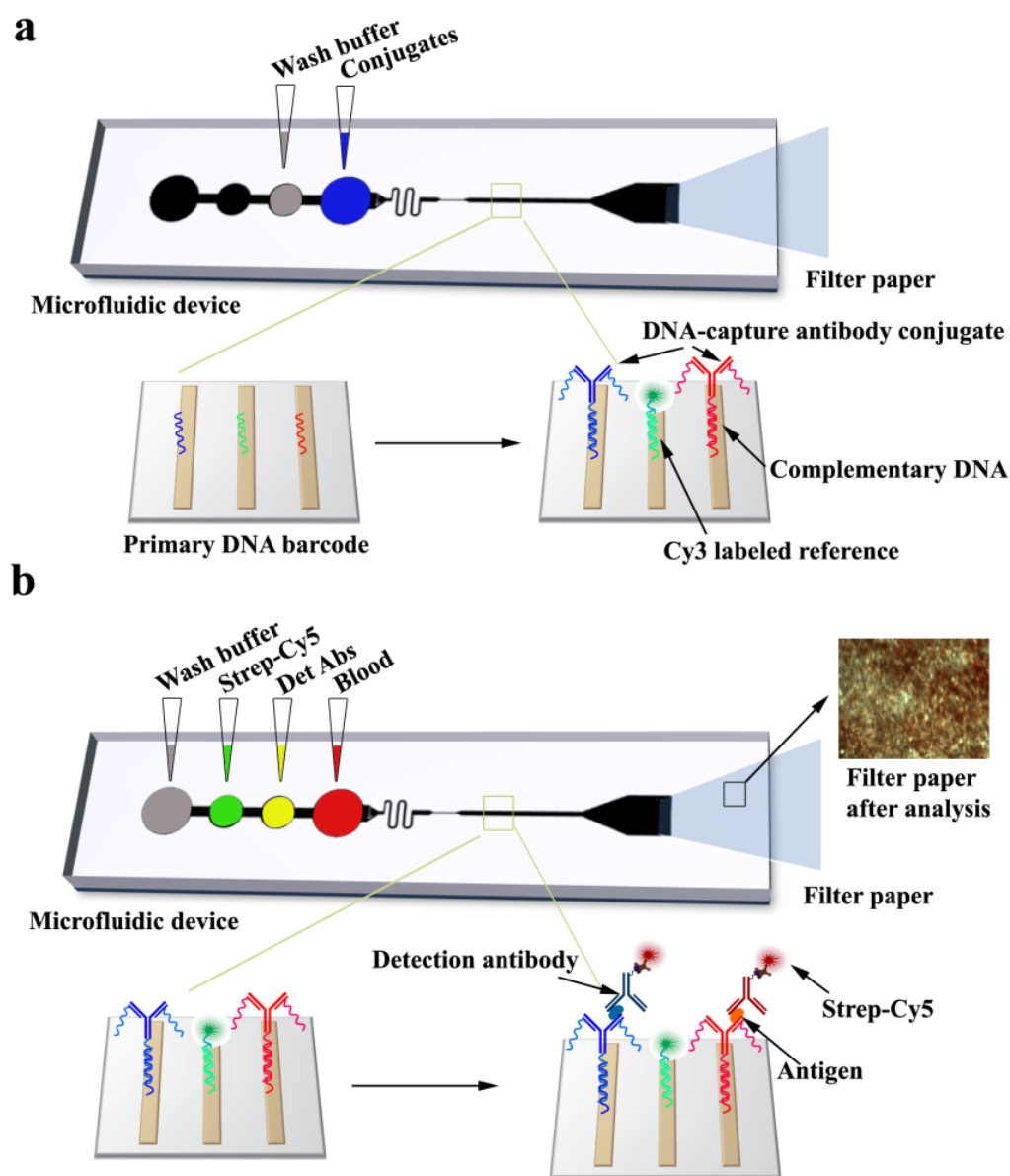
Supplementary Figures
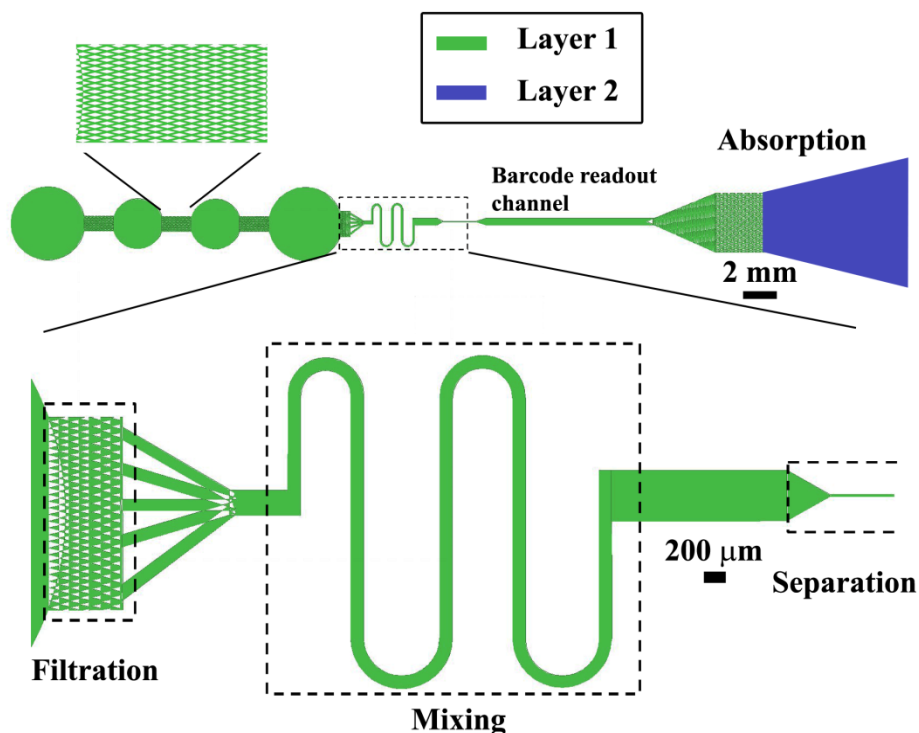
Supplementary Figure 1. Design of the LF-IBBC chip. The layout includes two layers, layer 1 for fluidic flow and layer 2 for filter paper insertion. All the chambers are connected by an array of posts which function as a filter to remove impurities and as a flow resistor. The minimum distance between posts in the last post array before the serpentine channel is designed to be 10 µm, which effectively dams large impurities and prevents clogging of the narrow, 12 µm channel ahead. The serpentine channel incorporates Dean vortices at each turn to mix solutions. The following narrow channel can effectively focus blood cells and separate them from plasma.
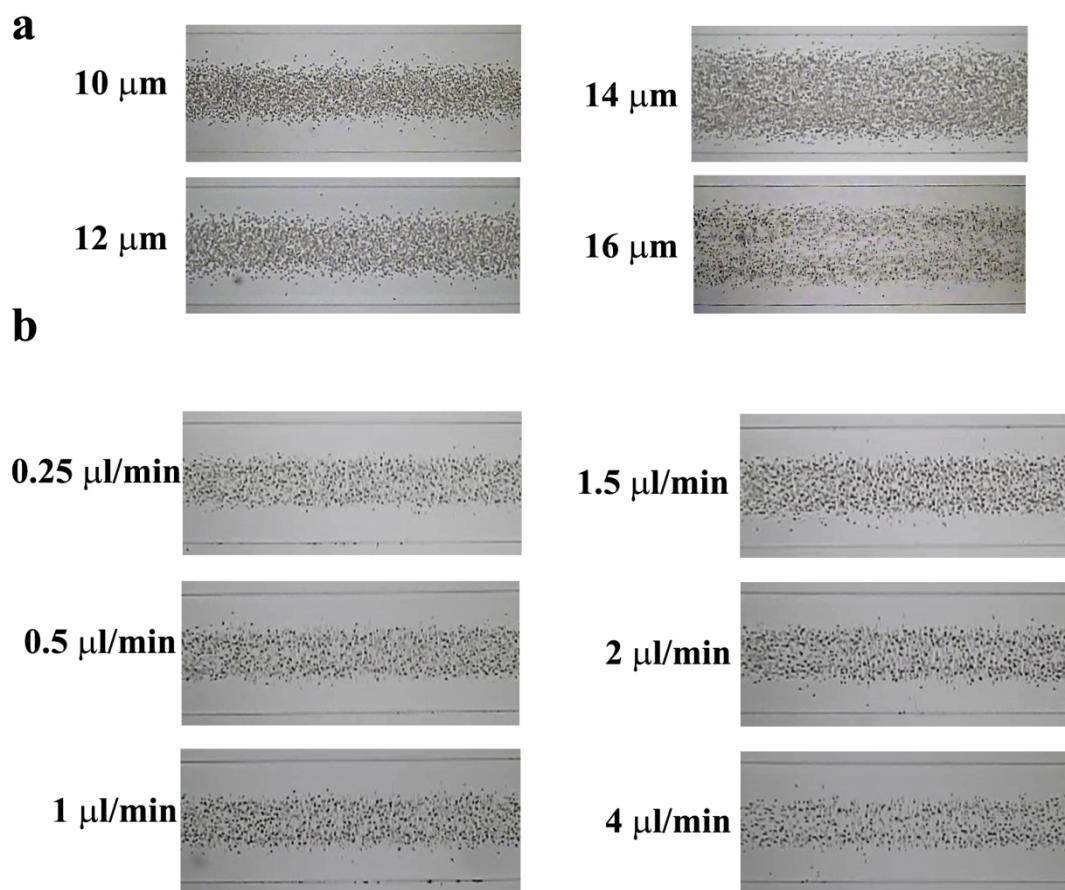
Supplementary Figure 2. Profile of flowing blood cells at barcode assay channel as a consequence of focusing at the narrow channel. **(a)** Effect of narrow channel width on cell focusing profile. (b) Effect of flow velocity on focusing profile when the narrow channel width was 12 μm. In the range between 0.25 μl/min and 4 μl/min, the flow velocity has negligible effect on blood cell focusing. The blood cells tend to be nonspecifically captured by stripes as well as the channel's bottom surface when the velocity is less than 0.5 μl/min.
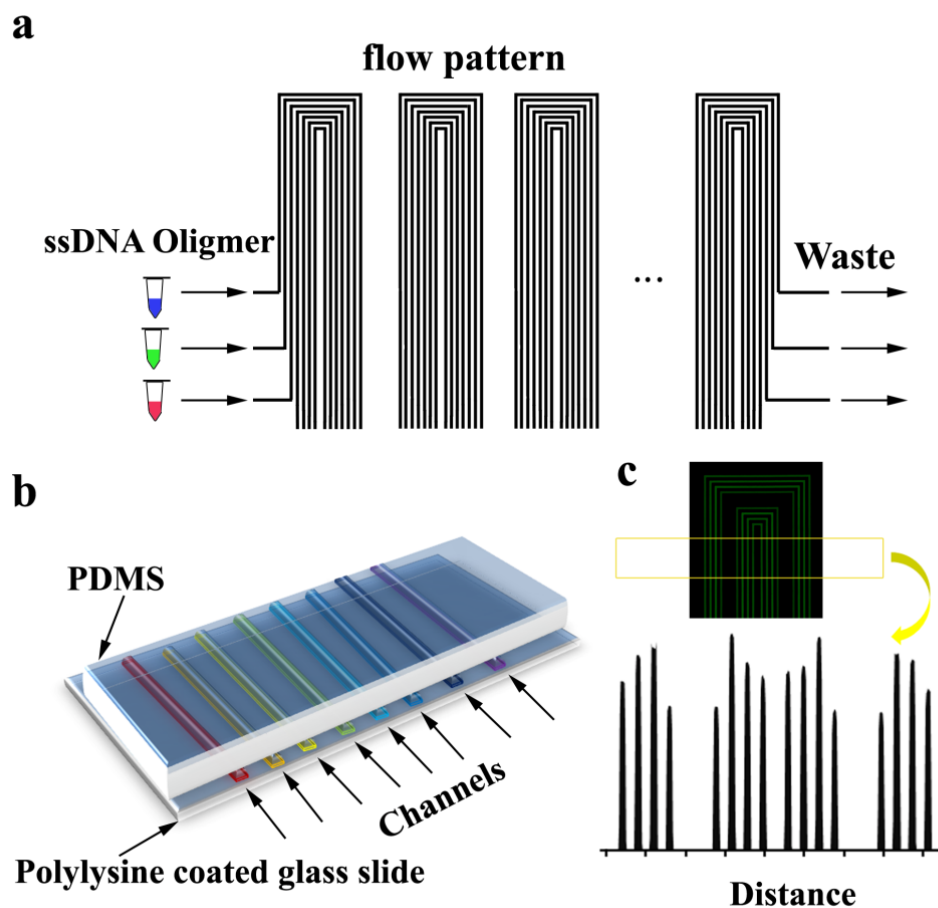
Supplementary Figure 3. Fabrication of DNA barcode array. High-density channels guide DNA oligomers to form a compact DNA array with as many as 36 replications shown in (a). The flow patterning is accomplished via the microfluidic device illustrated in (b), which is comprised of a PDMS replica bonded to a polylysine glass slide to seal the channels. Prior to conducting protein experiments, a section of each slide is tested with Cy3-labeled complementary DNA to confirm the presence and the quality of the DNA barcode as shown in (c). These DNA barcodes may be stored (under N_2) for at least 6 months without degradation.

Supplementary Figure 4. Procedure for LF-IBBC preparation and operation. (a) Preparation of the microchip: 10 µl DNA-antibody conjugates and 10 µl wash buffer (3% BSA in PBS) were added to their respective chambers as illustrated. Subsequently, the conjugates are assembled onto the DNA array via DNA hybridization. (b) Operation of a LF-IBBC for blood sample analysis: wash buffer, Strep-Cy5 (Streptavidin-Cy5), Det Abs (Detection antibodies) and blood

are added to their respective chambers, and filter paper is used to initiate flow. An ELISA sandwich structure is generated where the fluorescence intensity of each stripe indicates the amount of the corresponding protein concentration in blood.
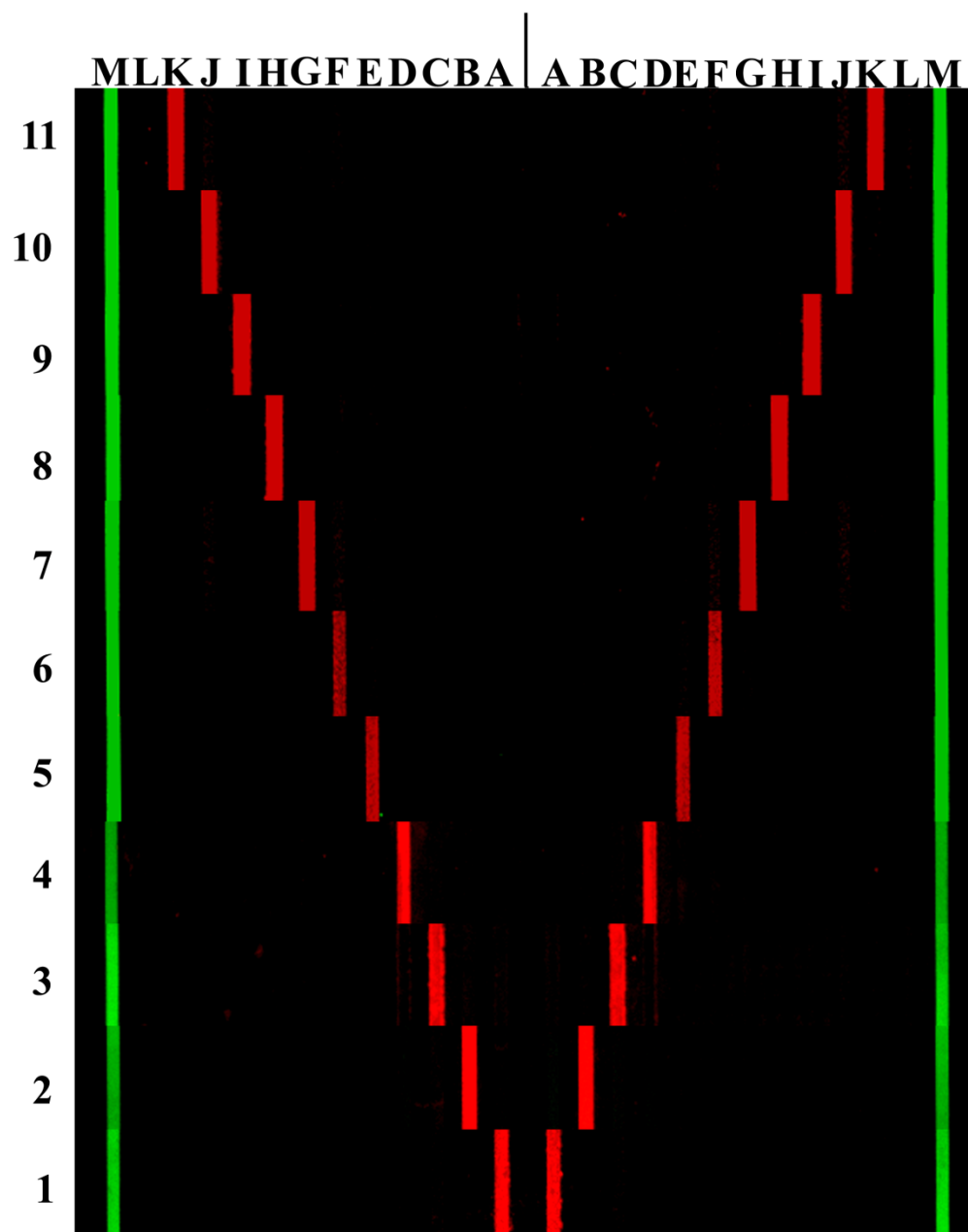
Supplementary Figure 5. Cross-reactivity of the multiplex protein assay. Only one recombinant protein at 10 ng/ml was present in each sample to be detected (row). The red stripes indicate

proteins detected. The green stripes are the references to spatially locate the red stripes and hence find the corresponding protein in Supplementary Table 2.
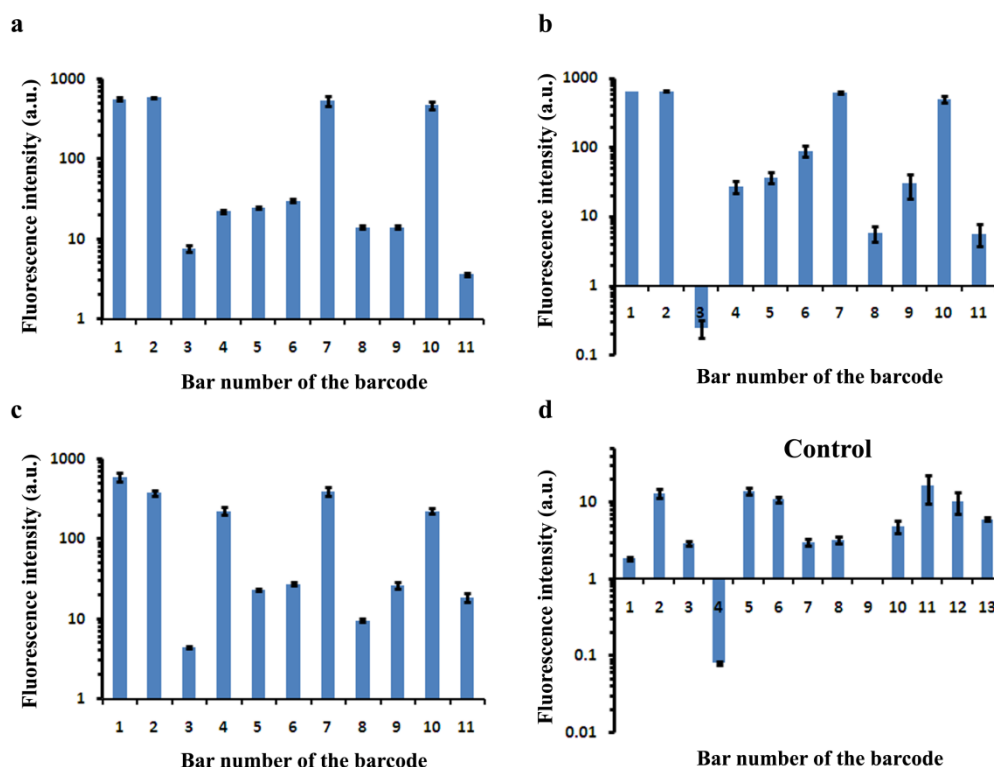
Supplementary Figure 6. (a-c) Quantified results of 3 blood samples from different donors analyzed by LF-IBBC 40 min assays. 8 repeated barcodes were averaged and the standard deviations were generated to present error bars. (d) The control values are obtained by performing the same procedure as (a-c) except that the DNA-encoded capture antibodies were not patterned in the microchip, and so only background binding to the DNA oligomers was observed. Note that the y-axis of this plot is significantly expanded over that used for the blood samples.

Supplementary Tables

Table 1. List of oligonucleotide sequences and terminal functionalization

Name	Sequence	T_m
A	5'- AAA AAA AAA AAA AAT CCT GGA GCT AAG TCC GTA-3'	57.9
A'	5' NH3- AAA AAA AAA ATA CGG ACT TAG CTC CAG GAT-3'	57.2
B	5'-AAA AAA AAA AAA AGC CTC ATT GAA TCA TGC CTA -3'	57.4
B'	5' NH3AAA AAA AAA ATA GGC ATG ATT CAA TGA GGC -3'	55.9
C	5'- AAA AAA AAA AAA AGC ACT CGT CTA CTA TCG CTA -3'	57.6
C'	5' NH3-AAA AAA AAA ATA GCG ATA GTA GAC GAG TGC -3'	56.2
D	5'-AAA AAA AAA AAA AAT GGT CGA GAT GTC AGA GTA -3'	56.5
D'	5' NH3-AAA AAA AAA ATA CTC TGA CAT CTC GAC CAT -3'	55.7
E	5'-AAA AAA AAA AAA AAT GTG AAG TGG CAG TAT CTA -3'	55.7
E'	5' NH3-AAA AAA AAA ATA GAT ACT GCC ACT TCA CAT -3'	54.7
F	5'-AAA AAA AAA AAA AAT CAG GTA AGG TTC ACG GTA -3'	56.9
F'	5' NH3-AAA AAA AAA ATA CCG TGA ACC TTA CCT GAT -3'	56.1
G	5'-AAA AAA AAA AGA GTA GCC TTC CCG AGC ATT-3'	59.3
G'	5' NH3-AAA AAA AAA AAA TGC TCG GGA AGG CTA CTC-3'	58.6
H	5'-AAA AAA AAA AAT TGA CCA AAC TGC GGT GCG-3'	59.9
H'	5' NH3-AAA AAA AAA ACG CAC CGC AGT TTG GTC AAT-3'	60.8
I	5'-AAA AAA AAA ATG CCC TAT TGT TGC GTC GGA-3'	60.1
I'	5' NH3-AAA AAA AAA ATC CGA CGC AAC AAT AGG GCA-3'	60.1
J	5'-AAA AAA AAA ATC TTC TAG TTG TCG AGC AGG-3'	56.5
J'	5' NH3-AAA AAA AAA ACC TGC TCG ACA ACT AGA AGA-3'	57.5

K	5'-AAA AAA AAA ATA ATC TAA TTC TGG TCG CGG-3'	55.4
K'	5' NH3-AAA AAA AAA ACC GCG ACC AGA ATT AGA TTA-3'	56.3
L	5'-AAA AAA AAA AGT GAT TAA GTC TGC TTC GGC-3'	57.2
L'	5' NH3-AAA AAA AAA AGC CGA AGC AGA CTT AAT CAC-3'	57.2
M	5'-Cy3-AAA AAA AAA AGT CGA GGA TTC TGA ACC TGT-3'	57.6
M'	5' NH3-AAA AAA AAA AAC AGG TTC AGA ATC CTC GAC-3'	56.9

All sequences were purchased from Integrated DNA Technology (IDT) and purified through high performance liquid chromatography (HPLC).

Table 2. Summary of antibodies and vendors

DNA label	Barcode sequence	Name	Primary antibody	Detection antibody	Recombinant
A'	1	CRP	Mouse IgG2B Mab* (R&D***)	Mouse IgG2B Mab (R&D)	Sigma
B'	2	MMP3	Goat IgG Pab** (R&D)	Goat IgG Pab (R&D)	R&D
C'	3	Serpin	Mouse IgG1 Mab (R&D)	Goat IgG Pab (R&D)	R&D
D'	4	G-CSF	Mouse IgG1 Mab (R&D)	Goat IgG Pab (R&D)	R&D
E'	5	MIF	Mouse IgG1 Mab (R&D)	Goat IgG Pab (R&D)	ProSpec
F'	6	EGF	Mouse IgG1 Mab (R&D)	Goat IgG Pab (R&D)	ProSpec
G'	7	CCL5	Mouse IgG1 Mab (R&D)	Goat IgG Pab (R&D)	R&D
H'	8	VEGF	Mouse IgG2B Mab (R&D)	Goat IgG Pab (R&D)	R&D
I'	9	IL 8	Mouse IgG1 Mab (Biolegend)	Mouse IgG1 Mab (Biolegend)	Biolegend
J'	10	IL-1 β	Mouse IgG2b Mab (Biolegend)	Mouse IgG1 Mab (Biolegend)	Biolegend
K'	11	IP10	Mouse IgG1 Mab (R&D)	Goat IgG Pab (R&D)	R&D
L'	12	Control	Mouse IgG1 Isotype control (R&D)	N.A.	

*   Mab: monoclonal antibody
**   Pab: polyclonal antibody
*** R&D: R&D Systems

Supplementary Videos

Supplementary video 1. Inertial focusing of blood cells when flowing at 0.25 µl/min powered by syringe pump. The width of narrow channel is 12 µm.

Supplementary video 2. Inertial focusing of blood cells when flowing at 0.5 µl/min powered by syringe pump. The width of narrow channel is 12 µm.

Supplementary video 3. Inertial focusing of blood cells when flowing at 1 µl/min powered by syringe pump. The width of narrow channel is 12 µm.

Supplementary video 4. Inertial focusing of blood cells when flowing at 1.5 µl/min powered by syringe pump. The width of narrow channel is 12 µm.

Supplementary video 5. On-chip plasma and cells separation powered by a filter paper. The width of narrow channel is 12 µm.

Supplementary video 6. Self-replacement of dyes imaged at the end of narrow channel. 3 dyes were loaded to the LF-IBBC device. The video was taken at a speed of 0.5 frame/ min.

Supplementary Methods

1. Microchip design and fabrication

The microchip design shown in Supplementary Fig. 1 fully integrates filtration, mixing, separation, detection and absorption in one chip. 4 chambers were designed to load at most 4 reagents for a complete ELISA assay as described in the text. They are connected by arrays of posts that increase flow resistance as well as filter impurities. The last post array is more compact to keep impurities originating in the chambers from clogging the narrow channel.

A serpentine channel following the post filter is designed to reduce possible concentration gradients within the assay channel cross section[1]. It is not designed to mix the reagents from the separate microchambers. Dean vortices are generated in the curvilinear channel to induce transverse flow, while only simple Poiseuille flow occurs in straight channels of the microchip, pointing outwards in the same direction of the channel centerline. Without the serpentine channel, the fluorescence intensity across the width of a barcode stripe was not always uniform. The following narrow channel with high aspect ratio is designed to separate plasma from blood cells through hydrodynamic focusing without sheath flow. The subsequent barcode readout channel incorporates the DNA-encoded antibody array to detect proteins of interest *in situ* by sandwich ELISA. At the end of the channel an array of posts with similar design is intended to increase resistance and facilitate connection to a filter paper through capillary flow.

In the initial test, we used PDMS instead of NOA 63 to fabricate microfluidic devices. PDMS is not a good final solution for the microchip, because O_2-plasma treated PDMS is difficult to remove from the glass slide, and such removal is necessary for the final fluorescence scanning step. The pre-cure PDMS mixture of part A and part B (10:1; RTV 615, General Electric) was poured to a master and incubated at 80 °C for 40 min. The cured PDMS was cut off from the master and punched for access holes. Afterward the PDMS replica was cleaned by rinsing with isopropyl and deionized (DI) water followed with blow dry. After subsequent treatment with oxygen plasma at 25 W for 100 s to render the surface hydrophilic, the PDMS replica was bonded immediately to a DNA patterned array slide where the pattern was oriented perpendicularly to the microchannel. Because the barcodes cover the entire glass slide surface, no alignment is required during the processes of fabrication. The fabrication process of NOA 63 can be found in the Materials and Methods. This material is clear, colorless, has a low fluorescence background, thermally-stable and intrinsically sticky to a glass slide. After UV exposure of NOA 63, the surface is rendered significantly more hydrophilic with stability for more than 1 month and with a contact angle of 40º [2-3]. This is sufficient to allow solutions to spontaneously fill microchannels via capillarity.

2. Cell focusing by inertial force

Wall-repulsive forces have not been recognized as important for particle alignment in small-scale microfluidic channels. When the channel size is reduced to a certain dimension, wall-

repulsive forces become prominent. In other publications, particles or cells are divided into at least two streams in the simplest straight channel by inertial forces, although complicated geometry designs have been introduced to focus particles into a single stream[4-5]. We incorporate the straight channel to separate plasma and cells not only because of the simplicity of design, and the resultant high separation efficiency but because it is robust and insensitive against perturbations to the flow conditions.
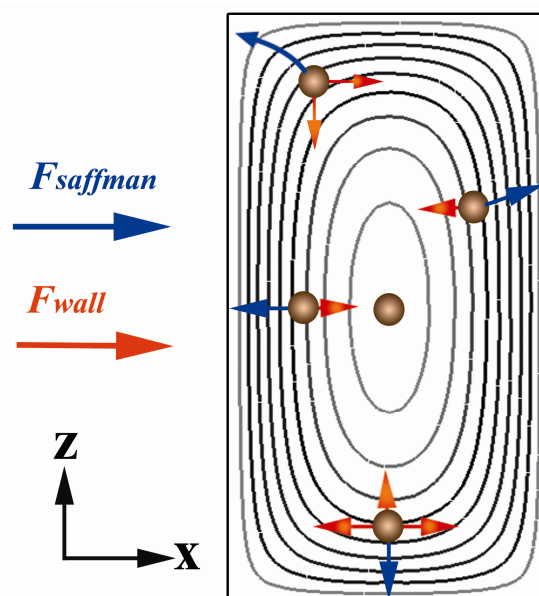
When a cell or particle is flowing through the narrow channel, it experiences wall-repulsive forces in a direction normal to the wall, and towards the microchannel center, due to stagnant flow close to the walls, as well as Saffman's lift force toward channel walls due to shear stress (Supplementary Fig. 7). The interaction of those forces determines the transverse migration of the particle in the microchannel cross-section. Presumably under our current channel design and flow condition, the magnitude of the wall-repulsive forces dominates all other forces (including the Magnus force due to free rotation), resulting in particles migrating to the microchannel center and focusing into a single stream when exiting the narrow channel.

As shown in Supplementary Fig.2, single stream focusing only occurs when the width of narrow channel is less than ~12 μm. When the width is expanded to 16 μm, the cell stream tends to be divided into two. We previously observed that spherical cells can be well focused in a single stream. In consideration of erythrocytes being concave-like and more deformable, this focusing is robust and likely more affected by the channel geometry. For further reproduction of inertial focusing on other cell types, the width of the channel should not exceed twice the cell diameter. Meanwhile the cross-section should have an aspect ratio > 1.5.

Supplementary Figure 7. Schematic illustration of inertial forces in the cross section of narrow channel. The particle at channel center has an equilibrium of lift forces.

3. Patterning barcodes

We improved the quality of ssDNA barcode array in terms of uniformity and density of ssDNA per unit area. ssDNA oligomers purchased from IDT were dissolved in a solution containing DI water and DMSO (2:1 v/v). High concentrations of ssDNA (here, 266 μM) yielded very dense DNA on each bar.

A different PDMS/glass slide hybrid device was fabricated first for flow patterning ssDNA. As described before, the PDMS replica was created according to standard soft lithography, followed by bonding of PDMS to a

polylysine glass slide with thermal treatment at 80 °C for 1 hr. Each channel of the microfluidic device was filled with a unique ssDNA sequence. The ssDNA filled microchip was then placed in a desiccator to allow solvent (water and DMSO) to evaporate from the channel. The entire microchip with deposited ssDNA left in the channels was incubated at 80 °C for 4 hours. This thermal process crosslinks ssDNA to the surface of polylysine glass slide. The slide was separated from the PDMS and subsequently cleaned by dipping with DI water to remove un-bonded ssDNA and other solids. Finally the slide was dried by N_2 blowing and preserved in a desiccator.

The compact antibody array was constructed by the DNA-encoded antibody library (DEAL) technique. For this method, DNA-conjugated antibodies are assembled onto the ssDNA array through complementary DNA hybridization (Supplementary Fig. 3 and Supplementary Fig. 4a)[6]. The ssDNA oligomers from A/A' to M/M' are optimized to be orthogonal to each other, ensuring one species of DNA linked antibody only localizes to a specific stripe with minimal cross-reactivity (Supplementary Table 1). Optimally, 3 strands of ssDNA linked to one antibody yields high affinity of the conjugate to pre-patterned complementary DNA without compromising antibody activity[6]. Sequence M is functionalized with M'-Cy3 as a reference, and provides registration for the remaining Cy5-labelled barcodes.

4. Operation of the LF-IBBC chip

The LF-IBBC is initially prepared by converting the DNA array into an antibody array through the introduction of the cocktail of DNA-encoded antibodies (Supplementary Fig. 4a). A slice of filter paper with the appropriate size was inserted into the slot in contact with the channel end. We chose the thinnest filter paper (grade 50, Whatman) with thickness of 115 μm because the hardened surface and the strong wettability are desirable as a component in our chip. The filter paper with 1.5 cm^2 can sustain wetting, and thus capillary-driven flow, for 2 hr. When we loaded wash buffer and DNA-antibody conjugates into the chambers, solutions filled all channels due to capillary force, within 5 min. Afterward the flow was supported capillarity from the filter paper. Once all solutions in the microchip were depleted, we stored the microchip in a 4 °C refrigerator.

To perform a one-step assay of whole blood, the microchip with the DNA-encoded antibody array provides the starting point. We first loaded 7 μl whole blood sample, 5 μl detection antibodies, 5 μl streptavidin-cy5 and 15 μl 3% BSA wt/v in PBS to chamber 4, 3,2 and 1, respectively (Supplementary Fig. 4b). The filter paper is then moved into the channel end, which immediately allowed fluidic flow to occur. For these concentrations of reagents and blood, a 40 min assay time is sufficient to completely drain all four chambers.

References

1. A. P. Sudarsan and V. M. Ugaz, *Proc. Natl. Acad. Sci. U S A*, 2006, **103**, 7228-7233.
2. S. H. Kim, Y. Yang, M. Kim, S. W. Nam, K. M. Lee, N. Y. Lee, Y. S. Kim and S. Park, *Adv. Funct. Mater.*, 2007, **17**, 3493-3498.
3. E. P. Dupont, R. Luisier and M. A. M. Gijs, *Microelectron. Eng.*, 2010, **87**, 1253-1255.
4. D. Di Carlo, D. Irimia, R. G. Tompkins and M. Toner, *Proc. Natl. Acad. Sci. U S A*, 2007, **104**, 18892-18897.
5. J. F. Edd, D. Di Carlo, K. J. Humphry, S. Koster, D. Irimia, D. A. Weitz and M. Toner, *Lab Chip*, 2008, **8**, 1262-1264.
6. R. C. Bailey, G. A. Kwong, C. G. Radu, O. N. Witte and J. R. Heath, *J. Am. Chem. Soc.*, 2007, **129**, 1959-1967.